



Seismicity patterns before MD ≥ 4.1 earthquakes in the Friuli-Venezia Giulia (northeastern Italy) and western Slovenia areas

Stefania Gentili, Gianni Bressan

► To cite this version:

Stefania Gentili, Gianni Bressan. Seismicity patterns before MD ≥ 4.1 earthquakes in the Friuli-Venezia Giulia (northeastern Italy) and western Slovenia areas. *Bollettino di Geofisica Teorica ed Applicata*, 2007, 48 (1), pp.33-51. inria-00403870

HAL Id: inria-00403870

<https://inria.hal.science/inria-00403870>

Submitted on 13 Jul 2009

HAL is a multi-disciplinary open access archive for the deposit and dissemination of scientific research documents, whether they are published or not. The documents may come from teaching and research institutions in France or abroad, or from public or private research centers.

L'archive ouverte pluridisciplinaire **HAL**, est destinée au dépôt et à la diffusion de documents scientifiques de niveau recherche, publiés ou non, émanant des établissements d'enseignement et de recherche français ou étrangers, des laboratoires publics ou privés.

Seismicity patterns before $M_D \geq 4.1$ earthquakes in the Friuli-Venezia Giulia (northeastern Italy) and western Slovenia areas

S. Gentili¹ and G. Bressan

Istituto Nazionale di Oceanografia e di Geofisica Sperimentale, Dipartimento Centro Ricerche
Sismologiche, Udine, Italy

Abstract – The spatial-temporal pattern of seismicity, preceding 5 moderate-sized earthquakes with $M_D \geq 4.1$, that occurred in the Friuli-Venezia Giulia region (northeastern Italy) and in western Slovenia, is investigated with the Region-Time-Length (RTL) and the PI algorithms. These algorithms were originally formulated to reveal the variation of seismicity patterns before large earthquakes.

The RTL algorithm detects seismic quiescences before the 1996 Claut earthquake (M_D 4.3), the 1998 Bovec earthquake (M_D 5.6), the 2002 Sernio earthquake (M_D 4.9) and the 2004 Bovec earthquake (M_D 5.1). No seismic quiescence is found before the 1988 Mena earthquake (M_D 4.1). A stage of foreshock activation is clearly observed only in the Claut case.

The PI method reveals space-temporal changes in the earthquake rate only before the Mena, Claut and Sernio earthquakes. The cases analyzed and those available in literature suggest that the seismicity anomalies like quiescence and foreshock activation preceding the moderate-sized events seem less evident than those preceding the severe earthquakes.

¹ Corresponding author: S. Gentili, Istituto Nazionale di Oceanografia e di Geofisica Sperimentale - Dipartimento Centro Ricerche Sismologiche, Via Treviso 55 - 33100 Cussignacco, Udine, Italy, Tel: +39 0432 522433, Fax: +39 0432 522474, e-mail: sgentili@inogs.it

1. Introduction

The analysis of the spatial and temporal patterns of seismicity has been widely used to investigate the earthquake preparation process. Many studies focussed on the quiescence that occurs during the phase of seismic energy accumulation before a severe earthquake. Temporal seismic observations have evidenced trends of seismic quiescences and foreshock activation preceding large events. The dilatancy hardening, over a broad region surrounding the nucleation zone of the impending earthquake, could be for Scholz (1988) the most important mechanism of the seismic quiescences. Wyss and Haberman (1988) attributed the occurrence of the seismic quiescences to the locking of the fault segments. Recently, Sobolev and Tyupkin (1996) developed the RTL (Region-Time-Length) algorithm to investigate the features of seismicity variations before strong earthquakes, consistent with laboratory experiments (Sobolev, 2000; Sobolev and Ponomarev, 2000). This approach takes into account the temporal, spatial and magnitude variation of seismicity around the site of the future earthquake, based on the assumption that a quiescence phase and foreshock activation precede the mainshock. The RTL algorithm was successfully applied to the seismicity preceding earthquakes with magnitude greater than 7.0 in the Kamchatka region (Sobolev, 2000), to earthquakes that occurred before the magnitude 7.2, 1995 Kobe earthquake (Huang et al., 2001) and to the seismicity before the magnitude 7.4, 1999 Izmit earthquake (Huang et al., 2002) and before the 2000 M=7.3 Tottori earthquake (Huang and Nagao, 2002). The RTL algorithm was also applied to Italian areas for minor magnitude earthquakes (Di Giovambattista and Tyupkin, 1999, 2000, 2004).

Recently, the PI (pattern informatics) technique was developed (Tiampo et al., 2001; Rundle et al., 2003) to recognize precursor seismic activation or quiescence for forecasting large earthquakes. The algorithm is based on the study of space-time fluctuations of a system to predict the future states. Nanjo et al. (2004) applied the PI technique to 18 earthquakes with magnitude ≥ 5 occurring from 1994 to 2004 in the Kobe area (Japan). Among the analyzed events there are the 1995 Kobe

earthquake (magnitude 7.2) and the Tottori event (magnitude 7.3). They found that 15 events occurred in the areas with $P' > 0$ or within 11 km of the epicenter. Rundle et al. (2003) obtained the forecast of five earthquakes with magnitude ranging from 5.1 to 5.7, that occurred from 2001 to 2003 in California using the same method. The September 21, 1999 earthquake of Taiwan (magnitude 7.6) is correctly forecasted with the PI algorithm by Chen et al. (2005).

In the present paper, the RTL and PI algorithms are used to analyze the seismicity patterns observed before the moderate earthquakes ($M_D \geq 4.1$) that occurred in the Friuli-Venezia Giulia region (Northeastern Italy) and in Western Slovenia. The purpose is to check the effectiveness of the methods applied to cases of moderate seismic events. The tectonic framework of the area is complex (see Fig. 1), resulting from the superposition of several Cenozoic-age tectonic phases (Venturini 1991). The main tectonic phases that affected the region were: the Mesoalpine NE-SW oriented compression (Middle-late Eocene), the Neoalpine N-S oriented compression (Middle Miocene-earliest Pliocene) and the Neoalpine NW-SE oriented compression (Pliocene). Each tectonic phase inherited and reactivated the main pre-existing faults and fragmented the crust into different tectonic domains (Bressan et al., 2003). The western part of the area is mainly affected by NE-SW—oriented thrusts and south-verging—thrusts. The main tectonic pattern in the central part of the area is formed by an E-W—trending system of south-verging—thrusts and folds, with a few backthrusts. Both western and central tectonic structures are intersected by strike-slip and normal faults, striking about NW-SE and NNE-SSW. NW-SE—trending strike-slip faults and thrust controls the tectonic pattern in the eastern part of the area.

We investigated the anomalies of seismicity preceding 5 earthquakes (fig. 1 and 2). The events are: the February 1, 1988 Mena earthquake (M_D 4.1), the April 13, 1996 Claut earthquake (M_D 4.3), the April 12, 1998 Bovec earthquake (M_D 5.6), here called Bovec98, the February 14, 2002 Sernio earthquake (M_D 4.9) and the July 12, 2004 Bovec earthquake (M_D 5.1), here called Bovec04. The duration magnitude of Rebez and Renner (1991) is considered for the whole database.

The seismicity in the Friuli-Venezia Giulia region and neighbouring areas was recorded by the local seismic network of the Istituto Nazionale di Oceanografia e Geofisica Sperimentale (OGS), that started to operate from May 7, 1977 with 7 stations. In 1982, the number of seismic stations was increased to 12. The present configuration of 16 stations, placed in the Friuli-Venezia Giulia region, was achieved in 1984. The earthquakes were located with a HYPO71 programme (Lee and Lahr, 1975). The seismicity recording was interrupted on December 3, 1990 and started again on May 21, 1991. The seismic data before January 1, 1988 were analogic. After this date the seismicity was acquired with digital signal processing (Gentile et al., 2000). The level of completeness magnitude from 1980 to 1990 and from 1991 to 2004 was found to be 2.0. No systematic change in magnitude, due to the different network configuration, or to the change from analogic to digital signals, was observed.

2. Methods

2.1 RTL algorithm

The RTL method was formulated by Sobolev and Tyupkin (1996) to investigate the space-temporal variation of seismicity preceding a large earthquake. In particular, the purpose of the RTL analysis is to detect the seismic quiescence occurring in the area around the future focus (test site) of a strong earthquake, during the phase of accumulation of the strain energy.

The RTL algorithm in a given test site (x, y) at time t , is defined as the product of the epicentral R , the temporal T and the source site L functions, divided by their standard deviation.

They are defined as follows:

Epicentral function:

$$R(x, y, t) = \sum_{i=1}^n \exp\left(-\frac{r_i}{r_0}\right) - R_s(x, y, t) \quad (1)$$

where r_i are the distances, between the tested point (x, y) and the i -th earthquake, of the n events considered in the time window $(t-2t_0, t)$, within a distance $2r_0$ from the tested point, with magnitude

in the interval (M_{min}, M_{max}) , with M_{min} the level of the catalogue completeness. The length $2t_0$ of the time window should be of the order or less than the duration of the seismic quiescence. M_{max} , r_0 and t_0 are chosen empirically. R decreases when the distances r_i increase or when the number of earthquakes decreases.

Time function:

$$T(x, y, t) = \sum_{i=1}^n \exp\left(-\frac{t-t_i}{t_0}\right) - T_s(x, y, t) \quad (2)$$

where t_i are the times of occurrence of the events preceding the tested earthquake. T decreases when the number of earthquakes in a time window before the time t decreases with respect to its mean.

Rupture length function:

$$L(x, y, t) = \begin{cases} \sum_{i=1}^n \left(\frac{l_i}{r_i}\right) - L_s(x, y, t) & \text{if } r_i > \varepsilon \\ \sum_{i=1}^n \left(\frac{l_i}{\varepsilon}\right) - L_s(x, y, t) & \text{if } r_i \leq \varepsilon \end{cases} \quad (3)$$

where ε is the accuracy of the epicenter location (Di Giovambattista and Tyupkin 2004) and l_i are the size of the source of the selected earthquakes as a function of magnitude. In this paper, the relation used by Di Giovambattista and Tyupkin (1999) (Papadopoulos and Voidomatis, 1987) is adopted:

$$\log(l_i) = 0.44M_i - 1.289$$

L decreases when the energy of the earthquakes in the area decreases, and/or when the higher energy earthquakes are located far from the tested point, and/or when the number of earthquakes decreases.

R_s , T_s , and L_s are linear trend corrections and they are normalized to a single variance. So the RTL parameter is measured in units of its variance.

RTL represents, substantially, the deviations from the background seismicity. The quiescence is marked by a decrease of the RTL parameter and the activation of seismicity is outlined by a growth of the RTL parameter. The RTL parameter is calculated after declustering aftershocks of the earthquake data set.

2.2 PI algorithm

The Pattern Informatics (PI) technique is an earthquake forecasting method based on the detection of precursory seismic activation or quiescence and has been applied to forecast earthquakes of magnitude 5 or greater (Nanjo et al. 2004, Rundle et al. 2003, Tiampo et al. 2001, Holliday et al. 2005a,b, Chen et al. 2005). The investigated area is divided into square cells (boxes) of size $\Delta x = 0.1^\circ \approx 11$ km. Unlike RTL, all the earthquakes over a given magnitude M_{min} (the magnitude of completeness of the data set) are considered, without declustering. Three times are considered: an initial time t_0 , from which the analysis is performed, a final time t_2 , after which the prevision will be made, and a time t_1 with $t_0 < t_1 < t_2$. The forecast interval is the time window (t_2, t_3) where $t_3 - t_2 \approx t_2 - t_1$ (Tiampo et al., 2001). The forecasted earthquakes have magnitude greater or equal to $M_{min} + 2$ (Holliday et al. 2005b). In order to account the arbitrary choice of where to center the boxes and the inaccuracies of the event location, the seismicity is averaged over each box and its eight surrounding boxes (Moore neighbourhood). The obtained time series are assigned to the central box.

The noise caused by areas characterized by low seismic activity is removed before applying the PI method. The number of earthquakes from t_0 to t_2 is calculated for each box and the PI method is applied only to the top 10 % most active boxes (Holliday et al., 2005b).

In the PI algorithm, the seismic intensity between two times t_b and t for each box, is defined as (Holliday et al., 2005b):

$$I(\vec{x}_i, t_b, t) = \frac{1}{t - t_b} \sum_{t'=t_b}^t N(\vec{x}_i, t_b, t') \quad (4)$$

where $N(\vec{x}_i, t_b, t')$ is the number of earthquakes in the i^{th} cell per unit time during the time interval (t_b, t') , i.e.:

$$N(\vec{x}_i, t_b, t') = \frac{n(\vec{x}_i, t_b, t')}{t' - t_b} \quad (5)$$

and n is the total number of earthquakes in the i^{th} box with magnitude greater than M_{min} in the time interval.

The measurement of the anomalous seismicity in a cell is performed by considering the two times, t_1 and t_2 :

$$\Delta I(\vec{x}_i, t_b, t_1, t_2) = I(\vec{x}_i, t_b, t_2) - I(\vec{x}_i, t_b, t_1) \quad (6)$$

In order to compare the intensities from different time intervals, and from one box to the other, the following matrices are evaluated:

$$\Delta \tilde{I}(\vec{x}_i, t_b, t_1, t_2) = \frac{\Delta I(\vec{x}_i, t_b, t_1, t_2) - \frac{1}{L} \sum_{t'=t_0}^{t_{max}} \Delta I(\vec{x}_i, t', t_1, t_2)}{\sqrt{\frac{1}{L} \sum_{t'=t_0}^{t_{max}} \left\{ \Delta I(\vec{x}_i, t', t_1, t_2) - \frac{1}{L} \sum_{t'=t_0}^{t_{max}} \Delta I(\vec{x}_i, t', t_1, t_2) \right\}^2}} \quad (7)$$

$$\Delta \hat{I}(\vec{x}_i, t_b, t_1, t_2) = \frac{\Delta \tilde{I}(\vec{x}_i, t_b, t_1, t_2) - \frac{1}{M} \sum_{i=1}^M \Delta \tilde{I}(\vec{x}_i, t_b, t_1, t_2)}{\sqrt{\frac{1}{M} \sum_{j=1}^M \left\{ \Delta \tilde{I}(\vec{x}_j, t_b, t_1, t_2) - \frac{1}{M} \sum_{i=1}^M \Delta \tilde{I}(\vec{x}_i, t_b, t_1, t_2) \right\}^2}} \quad (8)$$

where M is the number of cells, L is the number of time steps between t_0 and t_{max} and t_{max} is chosen equal to $t_1 - (t_2 - t_1)$ (Holliday et al. 2005a). In brief, the seismicity anomalies (seismic activity increase or quiescence) with time are stressed by $\Delta \tilde{I}(\vec{x}_i, t_b, t_1, t_2)$, while the space variation of seismicity is computed by $\Delta \hat{I}(\vec{x}_i, t_b, t_1, t_2)$. The variance expressed in the denominator of (7) and (8) is a normalization factor to weight less the boxes with high variability in time and space, respectively.

The average change intensity is calculated in order to reduce noise effects as:

$$\langle \Delta \hat{I} \rangle(\vec{x}_i, t_0, t_1, t_2) = \frac{1}{t_{\max} - t_0} \left| \sum_{t_b=t_0}^{t_{\max}} \Delta \hat{I}(\vec{x}_i, t_b, t_1, t_2) \right| \quad (9)$$

where $|\cdot|$ means absolute value.

The probability of change of activity in a cell is evaluated as:

$$P(\vec{x}_i, t_0, t_1, t_2) = \left\{ \langle \Delta \hat{I} \rangle(\vec{x}_i, t_0, t_1, t_2) \right\}^2 \quad (10)$$

since it is squared, unlike RTL, it measures both the seismic activation and seismic quiescence.

In order to detect which boxes will more likely be affected by a strong earthquake, the activation function is evaluated in comparison with the background obtaining:

$$P'(\vec{x}_i, t_0, t_1, t_2) = P(\vec{x}_i, t_0, t_1, t_2) - \frac{1}{M} \sum_{j=1}^M P(\vec{x}_j, t_0, t_1, t_2) \quad (11)$$

The cells with $P' > 0$ are the ones where a strong earthquake is predicted.

3. Results and discussion

3.1 RTL analysis

Figs. 3-7 show the plot of the RTL parameter computed at the epicentres of the Mena, Claut, Bovec98, Sernio and Bovec04 earthquakes, respectively, and the number of earthquakes with time, used in the RTL estimation. The temporal diagrams are constructed using a one-year moving time window with ten-day bins. The time of occurrence of the earthquakes is marked by an arrow.

The accuracy ϵ of the earthquake location is set at 2.0, considering that the average epicentral error location is 1.2 km. The minimum magnitude (completeness magnitude) is 1.2 for the Mena earthquake and 2.0 for the Claut, Sernio Bovec98 and Bovec04 cases. The model parameters are set as follows: $M_{\max} = 3.8$ and $t_0 = 0.5$ year, like Di Giovambattista and Tyupkin (1999), who performed the RTL analysis for tested shocks of moderate-sized magnitude; the radius r_0 is chosen

empirically equal to 20 km. As shown in Fig. 3a, the RTL algorithm fails in the case of the Mena earthquake. The quiescence detected from April 1982 to March 1983 appears too remote from the time of occurrence of the Mena episode, to be considered as its precursor. In the case of the Claut earthquake (Fig. 4a), a period of quiescence lasting from the end of September, 1995 to January, 1996 is recognizable. Then a phase of foreshock activation occurred, with main episodes M_D 3.5 (January, 27, 1996) and M_D 3.8 (February, 27, 1996).

The quiescence revealed by the RTL parameter before the Bovec98 case (Fig. 5a), started at the end of April 1995 and ended in the early days of December 1996. Then, an activation of seismicity (an increase of the RTL parameter) from March 1997 to March 1998 is detected.

Fig. 6a puts in evidence a period of quiescence from October 2001 to February, 14, 2002, the time of occurrence of the Sernio mainshock. The decrease of RTL before the Bovec04 mainshock (Fig. 7a) is less evident than in the other cases. We estimated its duration from January, 2003 to the time of the mainshock occurrence, July, 12, 2004. No relevant foreshock activation phases are detected in the Sernio and Bovec04 cases.

Huang (2006) analyzed the performances of the RTL method changing the model parameters for Tottori earthquake forecasting. He claimed that, if the performances are sensitive to the model parameters, some artifact can occur, and the detected quiescence can be only an artifact. In order to automatically detect changes of performances with different choices of parameters, he studied the possibility of a significant correlation existing in the corresponding RTLs at a significance level of 0.05 (Bendat and Piersol, 2000). If the significant correlation exists to the change of a parameter, the parameter does not affect the performances of RTL.

We claim that the Huang condition is sufficient, but not necessary to demonstrate the capability of the method to predict earthquakes, because only a decrease of the RTL before the earthquake and not a significant correlation with all the signal is needed for the prediction (see e.g. t_0 choice case for Bovec 2004, in the following). The cases where the Huang test fails should be analyzed independently.

Following the Huang approach, we tested RTL for different values of r_0 , i.e. 5, 10 and 20 km.

The results are presented in Table 1, where a significant correlation exists between $r_0=20$ km and $r_0=10$ km and $r_0=30$ km cases for all the earthquakes at a significance level of 0.05 (Bendat and Piersol, 2000). The correlation is generally smaller for $r_0=5$ km, and in some cases is not significant. No quiescence is detected in these cases for the RTL before the earthquake. Since Huang uses $r_0=50$ km and tested the method for $r_0=25$ and 100 km, and since in literature r_0 is set at 30-50 km (see e.g. Di Giovambattista and Tyupkin, 1999, 2000, 2004, Sobolev and Tyupkin, 1996, Sobolev 2000, Huang et al. 2002) we can hypothesize that there is a lower boundary under which the RTL is not able to predict earthquakes. This is not surprising, since no reliable RTL can be obtained if the event number is too small to ensure the statistics for calculating the RTL parameter. Thus no precursory quiescence and no significant correlation for $r_0=5$ km may be due to the insufficient number of earthquakes in this case.

The maximum magnitude of the earthquakes used for computing the RTL parameters is another parameter to be analyzed. Di Giovambattista and Tyupkin (2004) claimed that it has to be smaller than the magnitude of the tested main earthquake. Huang (2006) excluded the maximum threshold magnitude, Sobolev and Tyupkin (1997) set $M_{max} \approx M_{seq} - 2$, where M_{seq} is the magnitude of the tested main shock. Since we are investigating shocks with magnitude ranging from 4.1 to 5.6, poor statistics could result because the minimum magnitude is 2.0 for the Claut, Sernio and Bovec04 shocks and 1.2 for the Mena shock. Vice-versa, the M_D 5.6 Bovec98 case (completeness magnitude 2.0) remains unchanged, because no earthquake with magnitude greater than 3.0 was recorded before the main shock. In table 2, we present the correlation coefficients between the RTL calculated with $M_{max}=3.8$ (our choice) and the other choices of M_{max} . From Table 2, it emerges that a significant correlation exists between RTL obtained setting $M_{max}=3.8$ and $M_{max}=M_{seq}-2$ and M_{max} excluded, for all the earthquakes at a significance level of 0.05 (Bendat and Piersol, 2000). In particular, due to the small number of earthquakes with magnitude greater than 3.8 in our catalogue, the correlation coefficient of the RTL, for $M_{max}=3.8$ and eliminating M_{max} , is equal to 1.

The other questionable choice is the length $2t_0$ of the time window in the calculation of the RTL parameter. Di Giovambattista and Tyupkin (2004) claimed that the length $2t_0$ of the time window should be of the order or less than the duration of the seismic quiescence preceding the tested earthquake and that the quiescence phase of earthquake preparation can have a different duration for regions with different seismic activity.

In order to understand how the choice of the time window affects the results, we choose the length of time window $2t_0$ equal to those observed in the previous computed RTL parameter and perform the cross-correlation like in Huang (2006). So we set $2t_0$ equal to 7 months (Claut), 17.5 months (Bovec98), 4.5 months (Sernio) and 19 months (Bovec04). The case of Mena is not considered, because no quiescence phase is detected. The cross-correlation coefficient are presented in Table 3. From the table it emerges that a significant correlation exists between RTL obtained setting $t_0=0.5$ years and for the other choices for all the earthquakes at a significance level of 0.05 (Bendat and Piersol, 2000) except for Bovec 2004 RTL. This is due to differences in the previous part of the signal, but does not affect the capability of the method to detect earthquakes since the quiescence is observed (see Fig. 8). Therefore, we can say that also this parameter change does not affect the algorithm performances. In summary, all the parameter variations for $r_0 \geq 10$ km give rise to a RTL well correlated with the original one or, at least, to a detectable quiescence before the earthquake. In most cases a small correlation and no quiescence is detected for $r_0=5$ km. This is not surprising, since for small radii the statistic is poorer.

From the results obtained, we can conclude that the quiescence anomalies are not artifacts due to the choice of parameter.

We remark that the RTL algorithm was originally developed to investigate the spatial and temporal variation of seismicity patterns preceding large earthquakes (Sobolev and Tyupkin, 1996). The features of the seismicity patterns appear to be different from area to area, probably reflecting the different seismic regimes. Sobolev (2000), analyzed the precursory seismicity before three severe earthquakes that occurred in the Kamchatka region. The March 2, 1992 event with magnitude 7.1

was preceded by a quiescence that started 2.2 years before and lasted 1.7 years. A quiescence, that lasted 1.2 years, began 3 years before the magnitude 7.1 earthquake, that occurred on November 13, 1993. The December 5, 1997 event with magnitude 7.7 experienced a quiescence that started 3.7 years before and lasted 1.7 years. All these events were characterized by foreshock activation lasting 0.5, 1.8 and 1.7 years, respectively. Huang et al. (2002), found that the M_W 7.4 August 17, 1999 Izmit (Turkey) earthquake was preceded by a seismic quiescence starting about 2.5 years before and lasting about one year.

Di Giovambattista and Tyupkin (1999, 2000, 2004) analyzed the seismicity that occurred before moderate-strong earthquakes in different regions of Italy with the RTL algorithm. They found a quiescence period that started about 1.1 years before, lasted about 1 year, with a foreshock activation stage, prior to two earthquakes occurring on September 26, 1997 in the Umbria-Marche zone, with M_L 5.6 and M_L 5.8. The September 6, 2002 Palermo earthquake with magnitude 5.8 was characterized by a quiescence stage from November 2001 and lasted about 9 months. The quiescence period was not observed before three moderate earthquakes, with magnitude 4.9, 4.5 and 4.8, occurring in the Reggio Emilia area in 1983, 1987 and 1996, respectively. However, these earthquakes were preceded by the activation of weak earthquakes. In the previous tests, the quiescence appears in four cases, the Claut earthquake with M_D 4.3, the Bovec98 earthquake with M_D 5.6, the Sernio earthquake with M_D 4.9 and the Bovec04 event (M_D 5.1). The quiescence is less evident for the Bovec04 event and is absent before the Mena earthquake (M_D 4.1). An increase of seismic activity before the Bovec98 shock is noticeable from March 1997 to January 1998 and the foreshock activation is clearly observed only in the Claut case.

Results suggest that in cases of moderate earthquakes, like those analyzed in the present paper, the applicability of the RTL method is close to the limit. The quiescence stage, in the case of strong earthquakes, seems to start a longer time before and last longer than in the case of moderate earthquakes. In any case, the strong earthquake occurs after the RTL parameter is restored to its background level and is preceded by a stage of foreshock activation. These features are probably

less evident in the case of moderate earthquakes, as pointed out in the paper of Di Giovambattista and Tyupkin (1999).

Bufe and Varnes (1993) use precursory events to predict the time and the magnitude of mainshock events. They study earthquakes that exhibit accelerating seismic moment release (AMR), i.e. in terms of energy (Brehm and Braile 1998), in the selected area:

$$\sum \sqrt{E} = K - [k/m](t_f - t)^m$$

where $\sum \sqrt{E}$ is the cumulative square root of the seismic energy realized at time t , K is the cumulative square root of energy released, t_f is the time of failure and k and m are constants.

We calculate the cumulative sum of the square root of the seismic energy released with time (Fig. 9 a, b, c, d, e). However, no evident acceleration of the process is detected except in the case of the Claut event.

3.2 PI analysis

We set t_0 equal to the time when the available data set starts. The choice of time interval (t_0, t_1) and (t_1, t_2) affects the performances of the method. In literature, the time difference between t_0 and t_1 of the PI algorithm is variable. In particular, it is 6 years for the analysis of Taiwan seismicity (Chen et al., 2005) and 8 years in the study of Nanjo et al. (2004) on Japan seismicity. Tiampo et al. (2001), Rundle et al. (2003), Holliday et al. (2005a,b) adopted t_0 - t_1 ranging between 35 to 58 years in their studies on California earthquakes. The choice of the time difference between t_2 and t_1 is also variable and accounts for 6 years in the Taiwan case (Chen et al., 2005), ranges between 3–20 years in the California events analysis (Tiampo et al., 2001; Rundle et al., 2003; Holliday et al., 2005a,b) and is 26 years for Japan seismicity investigations (Nanjo et al., 2004).

As already pointed out in the introduction, the seismicity of the Friuli-Venezia Giulia region from December 3, 1990 to May 21, 1991 is not available because of the interruption of the seismic recording. After several tests, we found the best performances for $t_2 - t_3 = 1$ year. Thus, the time difference between t_0 and t_1 ranges from the 4 years for the forecast of the Claut earthquake to the

13 years for the forecast of the Bovec 2004 earthquake. We set $M_{min} = 2.0$, which is the completeness magnitude for the Friuli - Venezia Giulia region, in the considered period.

As already pointed out before, the method has been developed to forecast earthquakes with magnitude greater than 5. In addition, *“The PI method does not predict earthquakes, rather it forecasts the regions (hotspots) where earthquakes are more likely to occur in the relatively near future”* (Holliday et al., 2005b). This means that the PI method detects false alarms, since it indicates the cells where a strong earthquake most probably could occur, without saying if the earthquake will occur or not.

Another feature of the PI method is that, after a significant earthquake, the prevision for the corresponding cell is always positive (i.e. forecasts another earthquake), as pointed out by Tiampo et al. (2000). This is due to the fact that PI algorithm puts in evidence anomalies in the earthquake rate. The aftershocks of a strong earthquake always represent such an anomaly.

The results are presented in Fig. 10. The grey level corresponds to the value of $P' > 0$ (darker squares correspond to higher values), triangles correspond to earthquakes with magnitude greater than 2 between t_1 and t_2 and circles to earthquakes between t_2 and t_3 (the prediction time) with magnitude greater than 4.

Holliday et al. (2005b) considers the method to be successful if a significant event occurs in a hotspot box or within the Moore neighborhood of the box (i.e. the 8 boxes surrounding the box).

The Mena, Claut and Sernio earthquakes are correctly predicted (Fig. 10 a, b, d). In particular, one hotspot coincides with the Mena earthquake, while the other two earthquakes have a hotspot in their surrounding. The cells where these earthquakes are located are characterized by a slight quiescence of seismic activity. The two Bovec earthquakes, that are the ones with higher intensity, are not predicted (Fig. 10 c, e). The Bovec98 event occurs in a box which is not in the top 10% most active cells while the cell where the Bovec04 event is located has negative P' . The reason for the failure of the method is probably due to the fact that the events occur on the border of the area covered by the seismic network. The method involves computing of the seismic activity of the tested box (the

box where the significant earthquake occurs) with respect to other surrounding boxes. In these cases, the eastern boxes are not covered by the seismic network and consequently the seismicity is poorly detected.

4. Conclusions

The analysis of the seismicity preceding 5 moderate-magnitude earthquakes, located in the Friuli-Venezia Giulia region (northeastern Italy) and western Slovenia, has shown the following space-temporal aspects.

Seismic quiescence, investigated with the RTL method, appears before the Claut earthquake (M_D 4.3), the Bovec98 earthquake (M_D 5.6), the Sernio earthquake (M_D 4.9) and the Bovec04 event (M_D 5.1). Seismic quiescence is not detected prior the Mena earthquake (M_D 4.1).

The April 13, 1996 Claut earthquake (M_D 4.3) was preceded by a quiescence that started about 7 months before and lasted about 4 months. The April 12, 1998 Bovec earthquake (M_D 5.6) was preceded by a quiescence that started about 2 years and 8 months before and lasted 17 months. A phase of activation of weak earthquakes occurred from April 25, 1997 to February 15, 1998. The February 14, 2002 Sernio earthquake (M_D 4.9) was preceded by a quiescence that started about 4.5 months before and lasted till the mainshock. The July 12, 2004 Bovec earthquake (M_D 5.1) was preceded by a quiescence that started about 19 months before and lasted till the occurrence of the mainshock. The quiescence preceding the Bovec04 event is less evident than in the other cases, with a slow decrease of the RTL parameter. The Sernio and Bovec04 events occur at the end of the quiescence, without restoring the RTL parameter to its background level. A marked foreshock activation is observed only in the Claut case, manifested by an acceleration of the seismic energy release.

The RTL parameter does not vary significantly if values of M_{max} , t_0 and r_0 (with $r_0 \geq 10\text{km}$) different from those traditionally adopted, are used in the algorithm. So the choice of $M_{max} = 3.8$ and $t_0 = 0.5$

year seems suitable. The best choice for the distance (radius) including the analyzed seismicity with respect to the tested point (earthquake to forecast), is 20 km.

The PI algorithm reveals anomalies in the earthquake rate in the Mena, Claut and Sernio cases. It fails in the cases of the Bovec earthquakes, probably because the tested events are located outside the area covered by the seismic network and the seismicity in the zones around their location is poorly detected. The PI method is essentially based on measuring the earthquake rate of the tested box with respect to that of the other surrounding boxes. In any case, false alarms are detected.

The statistics are too few to make any general consideration about the seismic anomalies preceding the moderate-sized magnitude events and the reliability of the methods to detect them here. However, the analyzed cases and those quoted in literature suggest that the seismicity anomalies like quiescence and foreshock activation, preceding the moderate-sized events, seem less evident than those preceding the severe earthquakes. The PI algorithm appears less fair than the RTL algorithm to reveal the variation of the seismicity patterns preceding the moderate earthquakes, here considered. A reason could be that, at least for the analyzed cases, it is not sufficient to consider only the variation in the earthquake rate, but it is also necessary to account for the variation of the earthquake energy, as provided in the RTL algorithm.

Acknowledgements

The local seismic network is managed by the Dip. Centro di Ricerche Sismologiche of Istituto Nazionale di Oceanografia e Geofisica Sperimentale (OGS) with the financial contribution of the Regione Friuli-Venezia Giulia. We thank the technical staff for data acquisition.

5. References

- Bendat, J. S. and Piersol, A. G.; 2000: *Random Data: Analysis and Measurements Procedures*. 2nd Edition John Wiley and Sons eds.
- Brehm, D. J., and Braile, L. W.; 1998: *Intermediate-term Prediction Using Precursory Events in the New Madrid Seismic Zone*. Bull. Seismol. Soc. Am. **88**, 564–580.
- Bressan G., Bragato P.L. and Venturini C.; 2003: *Stress and strain tensors based on focal mechanisms in the seismotectonic framework of the Friuli–Venezia Giulia region (Northeastern Italy)*. Bull. Seism. Soc. Am., **93**, 1280-1297.
- Bufe, C. G. and Varnes, D. J.; 1993: *Predictive Modeling of the Seismic Cycle of the Greater San Francisco Bay Region*. J. Geophys. Res. 98, 9871–9883.
- Chen C.C., Rundle J.B., Holliday J., Nanjo K. and Li S.C.; 2005: *The 1999 Chi-chi Taiwan earthquake as a typical example of seismic activation and quiescence*. Geophys. Res. Letters, **32**, L22315.
- Di Giovambattista R. and Tyupkin Yu. S.; 1999: *The fine structure of the dynamics of seismicity before $M \geq 4.5$ earthquakes in the area of Reggio Emilia (Northern Italy)*. Annali di Geofisica, **42**, 897-909.
- Di Giovambattista R. and Tyupkin Yu. S.; 2000: *Spatial and temporal distribution of the seismicity before the Umbria-Marche September 26, 1997 earthquakes*. Journal of Seismology, **4**, 589-598.
- Di Giovambattista R. and Tyupkin Yu. S.; 2004: *Seismicity patterns before the $M=5.8$ 2002, Palermo (Italy) earthquake: seismic quiescence and accelerating seismicity*. Tectonophysics, **384**, 243-255.
- Gentile G. F., Bressan G., Burlini L., and De Franco R.; 2000: *Three – dimensional V_p and V_p/V_s models of the upper crust in the Friuli area (Northeastern Italy)*. Geophys. Journ. Int., **141**, 457-478.

- Holliday J. R., Nanjo K. Z., Tiampo K. F., Rundle J. B. and Turcotte D. L.; 2005a, *Earthquake forecasting and its verification*, Nonlin. Proc. Geophys., **12**, 965-977.
- Holliday, J. R., Chen C. C., Tiampo K. F., Rundle J. B. and Turcotte D. L.; 2005b: *A RELM earthquake forecast based on Pattern Informatics*. Seism. Res. Lett., in review 2005 .
- Huang, Q.; 2006: *Search for reliable precursors: A case study of the seismic quiescence of the 2000 western Tottori prefecture earthquake*. J. Geophys. Res., **111**, B04301, doi:10.1029/2005JB003982.
- Huang, Q., and Nagao, T.; 2002: *Seismic quiescence before the 2000 M=7.3 Tottori earthquake*. Geophys. Res. Lett., 29, 1578, doi: 10.1029/2001GL013835.
- Huang Q., Sobolev G. A. and Nagao T.; 2001: *Characteristics of the seismic quiescence and activation patterns before the M=7.2 Kobe earthquake*. Tectonophysics, **337**, 99-116.
- Huang, Q., Öncel A. O. and Sobolev G. A.; 2002: *Precursory seismicity changes associated with the Mw=7.4 1999 August 17 Izmit (Turkey) earthquake*. Geophys. J. Int., **151**, 235-242.
- Lee W. H. K. and Lahr J. C.; 1975: *HYP071 (revised): a computer program for determining hypocenter, magnitude and first motion pattern of local earthquakes*. U.S. Geol. Surv., Open File Rep. 75-311.
- Nanjo K. Z., Rundle J. B., Holliday J. R., Turcotte D. L.; 2004: *Pattern Informatics and Its Application for Optimal Forecasting of Large Earthquakes in Japan*. Submitted to Pure and Applied Geophysics.
- Papadopoulos, G. A. and Voidomatis P.; 1987: *Evidence of periodic seismicity in the inner Aegean seismic zone*. Pageoph, **125**, 613-628.
- Rebez, A. and Renner G.; 1991: *Duration magnitude for the northeastern Italy seismometric network*. Boll. Geof. Teor. Appl., **33**, 177-186.
- Rundle J. B., Turcotte D. L., Shcherbakov R., Klein W., Sammis, C.; 2003: *Statistical physics approach to understanding the multiscale dynamics of earthquake fault systems*. Reviews of Geophysics, **41**, 4, 1019.

- Scholz C. H.; 1988: *Mechanisms of seismic quiescences*. Pure and Applied Geophysics, **126**, 701-718.
- Sobolev G. A.; 2000: *Precursory Phases of large Kamchatkan Earthquakes*. Volc. Seis., **21**, 495-509.
- Sobolev G. A. and Tyupkin Yu. S.; 1996: New method of intermediate-term earthquake prediction
In: Seismology in Europe. ESC, Reykjavik, Iceland. pp. 229-234.
- Sobolev G. A. and Tyupkin Yu. S.; 1997: *Precursory Phases, seismicity precursors and earthquake prediction in Kamchatka*. Volc. Seis. **18**, 433-446.
- Sobolev G. A. and Ponomarev A. V.; 2000: *Acoustic emission and the precursory phases of failure in a laboratory experiment*. Volc. Seis. **21**, 479-496.
- Tiampo K. F., Rundle J. B., McGinnis S. and Gross S. J.; 2000: *Eigenpatterns in southern California seismicity* Rundle J. B., Turcotte, D. L. and Klein, W. eds., Geocomplexity and the Physics of Earthquakes, Geophysical Monograph Ser. 120, (American Geophysical Union, Washington, DC), pp. 211-218.
- Tiampo K. F., Rundle J. B., McGinnis S., Gross S. and Klein W.; 2001: *The Phase Dynamics of Earthquakes: Implications for Forecasting in Southern California*. <http://arxiv.org/abs/cond-mat/0102032>
- Venturini C.; 1991: *Cinematica neogenico-quadernaria del Sudalpino orientale (settore friulano)*. Studi Geol. Camerti, Vol. Spec., pp109-116.
- Wyss M. and Habermann R. E.; 1988: *Precursory seismic quiescence*. Pure and Applied Geophysics, **126**, 701-718.

Figure Captions

Fig 1: Schematic tectonic map of the northeastern Italy and Western Slovenia; line and dashed line: subvertical fault, toothed line: thrust. The location of the moderate-size earthquakes considered in the present study are marked with different symbols; full circle: 1996 Claut mainshock, full triangle: 2002 Sernio mainshock, asterisk: 1988 Mena mainshock, full square: 1998 and 2004 Kobarid mainshocks. BL: Belluno town; PN: Pordenone town; UD: Udine town; GO: Gorizia town; TS: Trieste town. Longitude-degrees (horizontal axis), latitude-degrees (vertical axis).

Fig 2: Friuli Venezia Giulia map with the epicenters of the earthquakes analyzed. Full inverted triangles represent the positions of the seismological stations of the Friuli Venezia Giulia network. Open inverted triangles represent the Slovenian seismic stations used to detect Bovec earthquakes.

Fig 3: Temporal variation of the RTL parameter calculated in the epicenter of the M_D 4.1 Mena earthquake (a). Number of earthquakes per year (b). The time of the occurrence of the tested earthquake is marked with an arrow.

Fig 4: Temporal variation of the RTL parameter calculated in the epicenter of the M_D 4.3 Claut earthquake (a). Number of earthquakes per year (b). The times of the occurrence of the two main foreshocks, with M_D 3.5 and M_D 3.8 and of the tested earthquake are marked with an arrow.

Fig 5: Temporal variation of the RTL parameter calculated in the epicenter of the M_D 5.6 Bovec98 earthquake (a). Number of earthquakes per year (b). The time of the occurrence of the tested earthquake is marked with an arrow.

Fig 6: Temporal variation of the RTL parameter calculated in the epicenter of the M_D 4.9 Sernio earthquake (a). Number of earthquakes per year (b). The time of the occurrence of the tested earthquake is marked with an arrow.

Fig 7: Temporal variation of the RTL parameter calculated in the epicenter of the M_D 5.1 Bovec04 earthquake (a). Number of earthquakes per year (b). The time of the occurrence of the tested earthquake is marked with an arrow.

Fig 8: Temporal variation of the RTL parameter for the M_D 5.1 Bovec04 earthquake with $2t_0$ equal to 19 months. The time of the occurrence of the tested earthquakes is marked with an arrow.

Fig 9: Cumulative sum of the square root of the seismic energy released with time by events preceding the main shocks (open circles): the M_D 4.1 Mena earthquake (a); the M_D 4.3 Claut earthquake (b); the M_D 5.6 Bovec98 earthquake (c); the M_D 4.9 Sernio earthquake (d); the M_D 5.1 Bovec04 earthquake (e).

Fig 10: Performances of the PI method for the forecasting of Mena (a); Claut (b); Bovec 1998 (c); Sernio (d) and Bovec 2004 (e) earthquakes. Only cells with $P' > 0$ are shown. The grey level corresponds to the value of P' (darker squares correspond to higher values), triangles correspond to earthquakes with magnitude greater than 2 between t_1 and t_2 and circles to earthquakes between t_2 and t_3 (the prediction time) with magnitude greater than 4.

Table Captions

Table 1: Correlation among RTL values with different choices of r_0 . In the case of Bovec98 too few data were available to calculate the *RTL*.

Table 2: Correlation among *RTL* values with different choices of M_{max} . $M_{max}=\infty$ means that the M_{max} has been eliminated.

Table 3: Correlation among RTL values with different choices of t_0 .

Figures

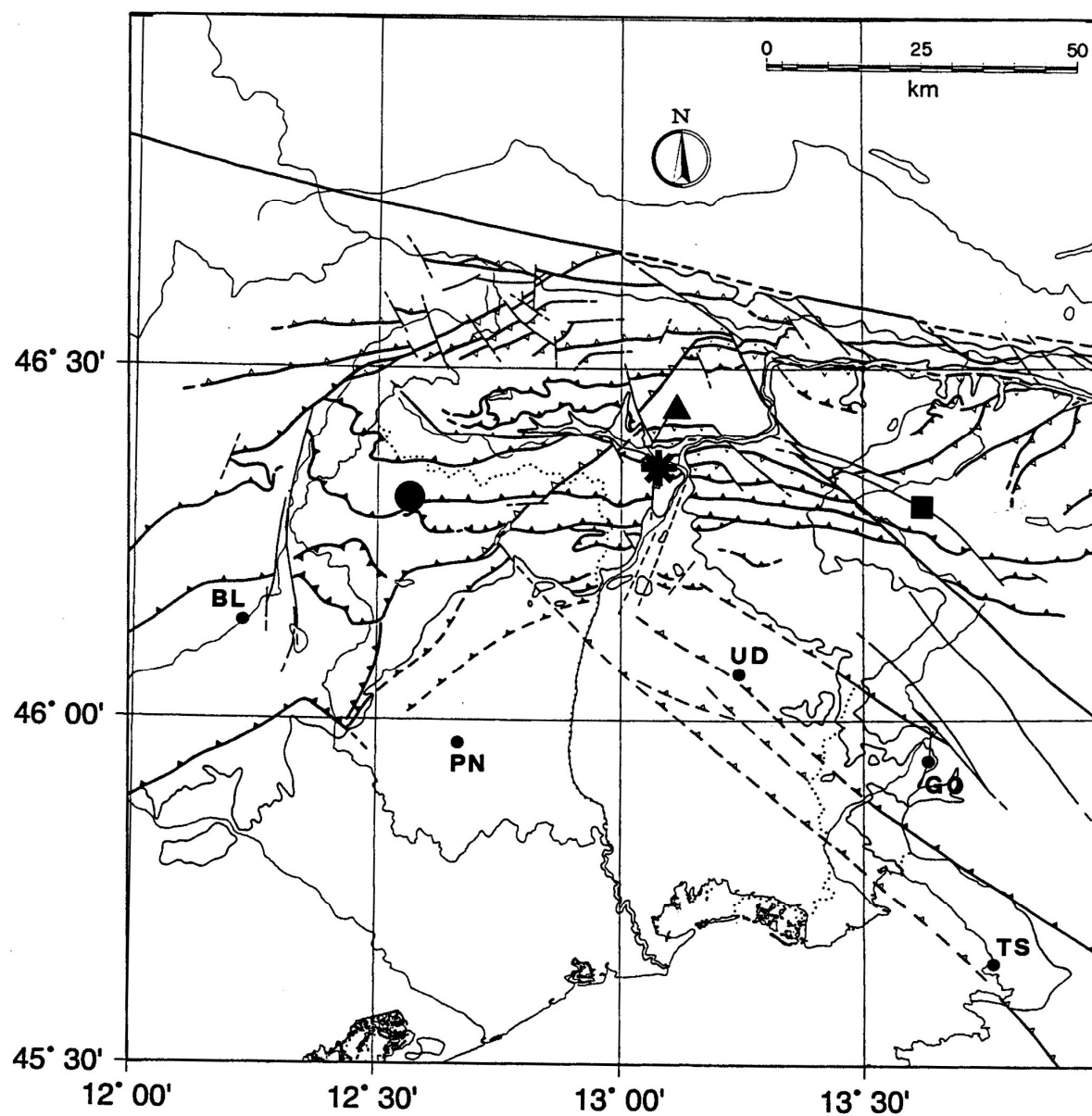


Fig 1

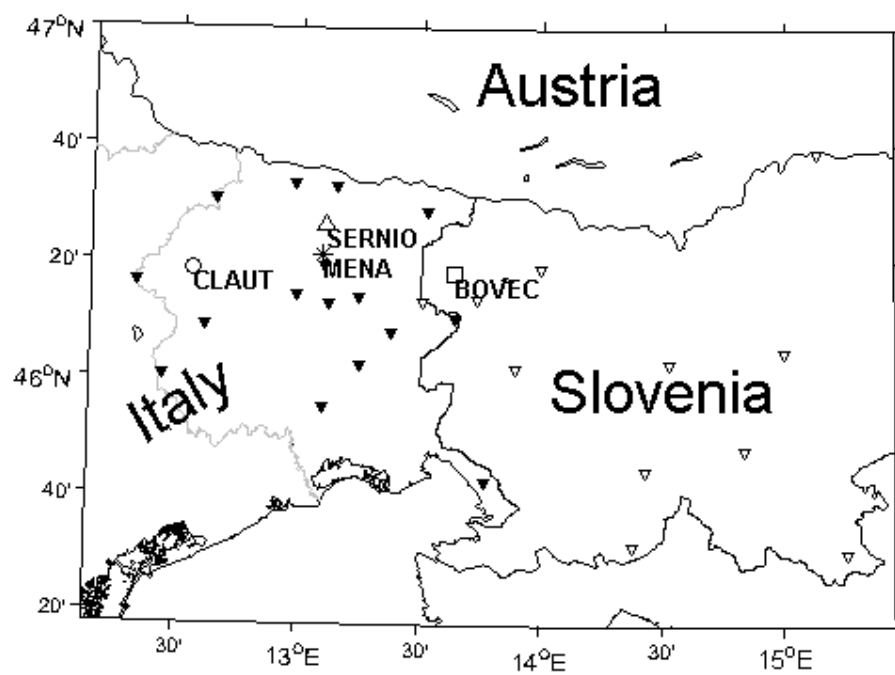
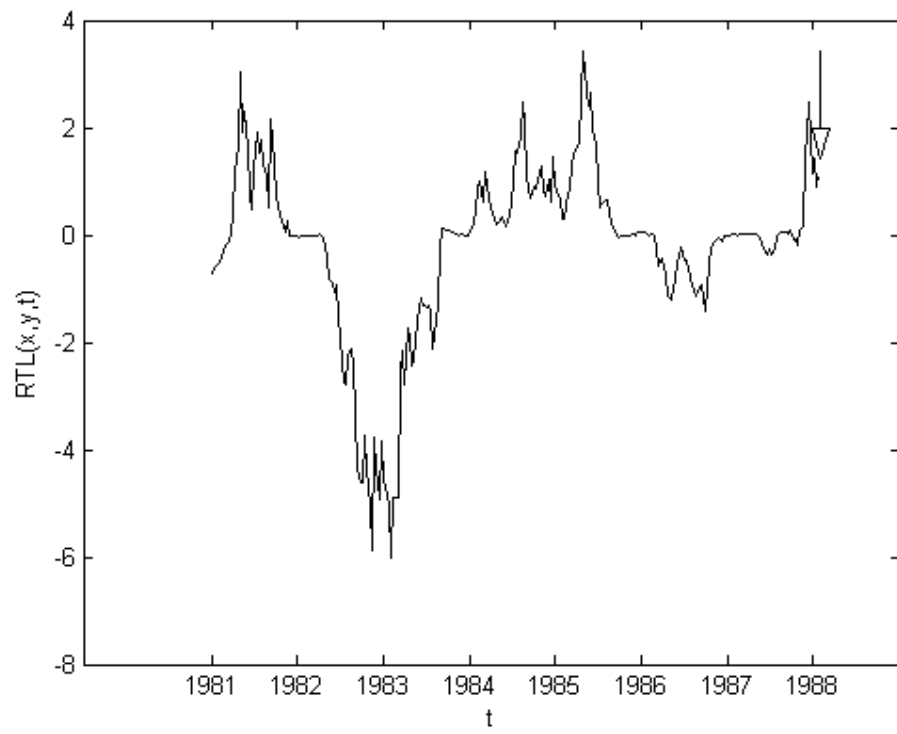
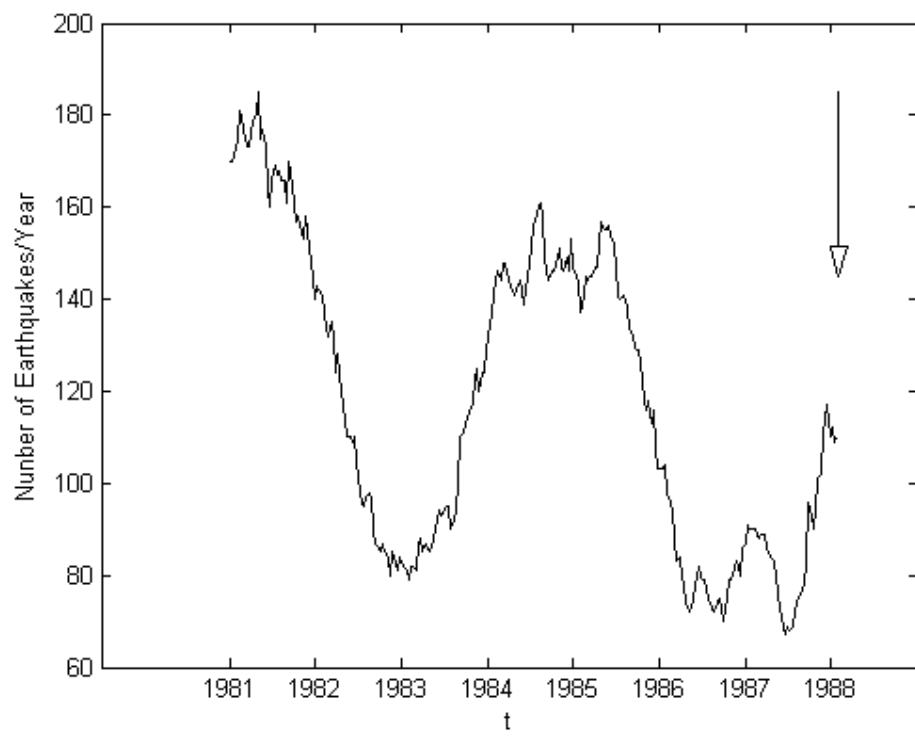


Fig. 2

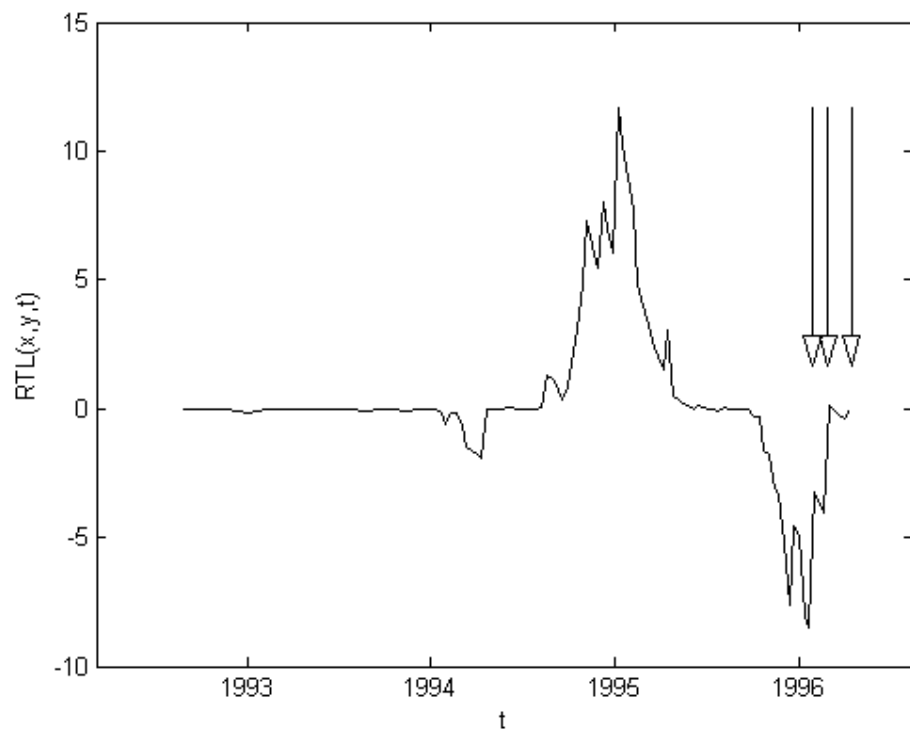


(a)

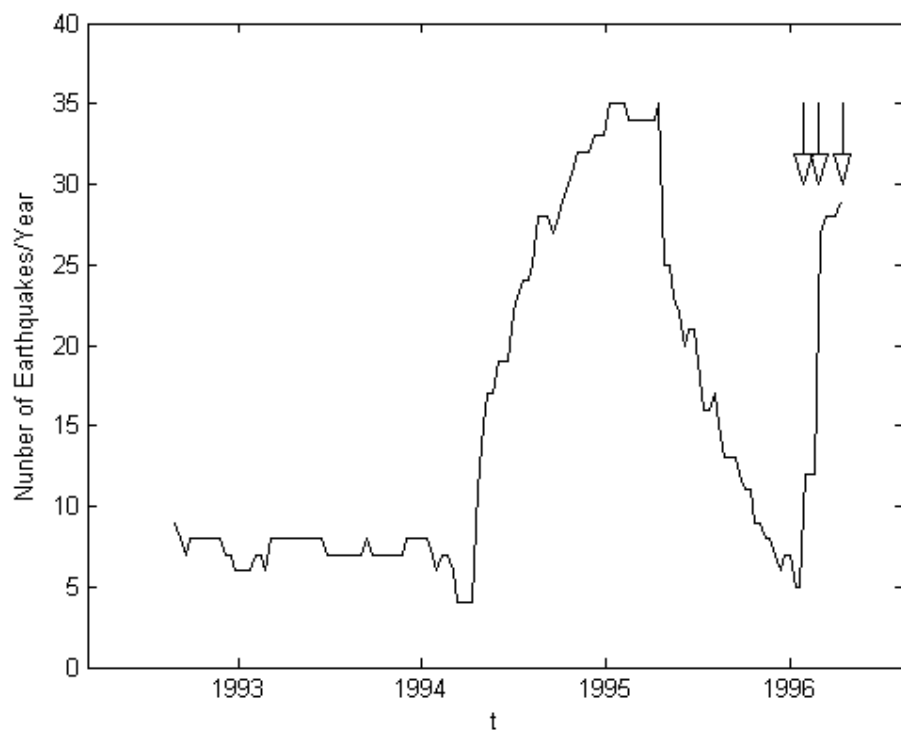


(b)

Fig. 3

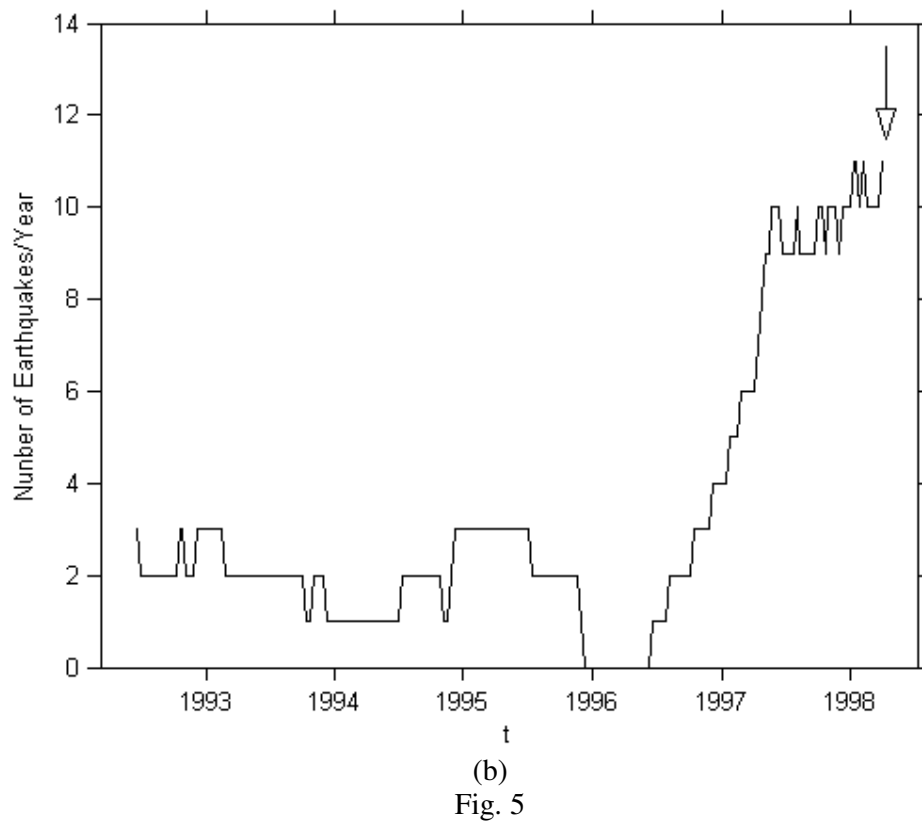
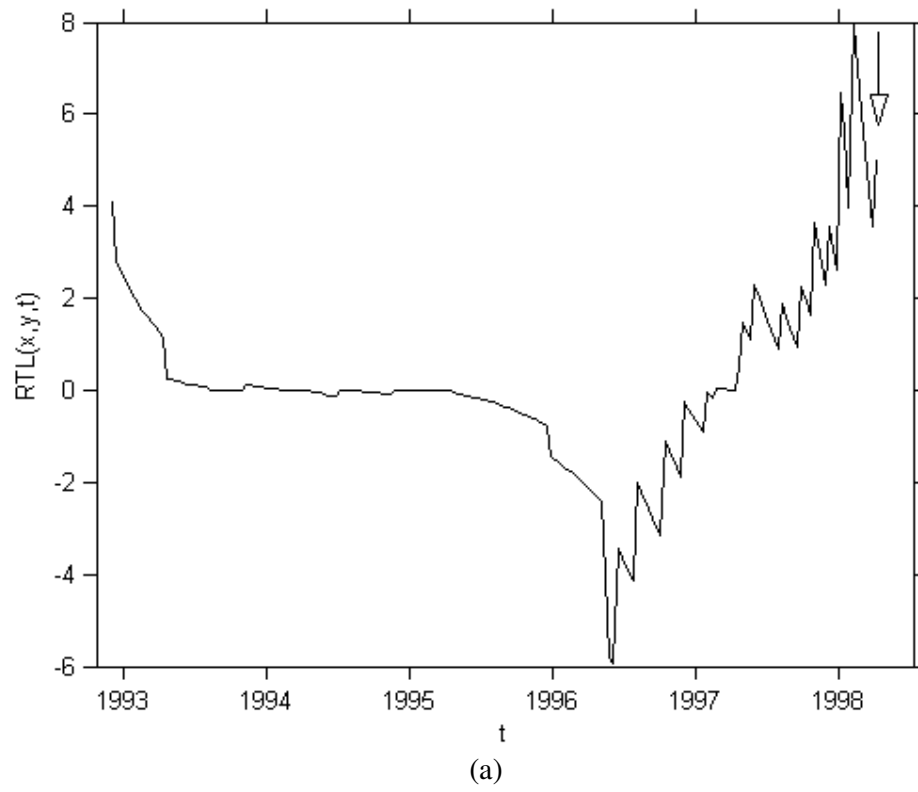


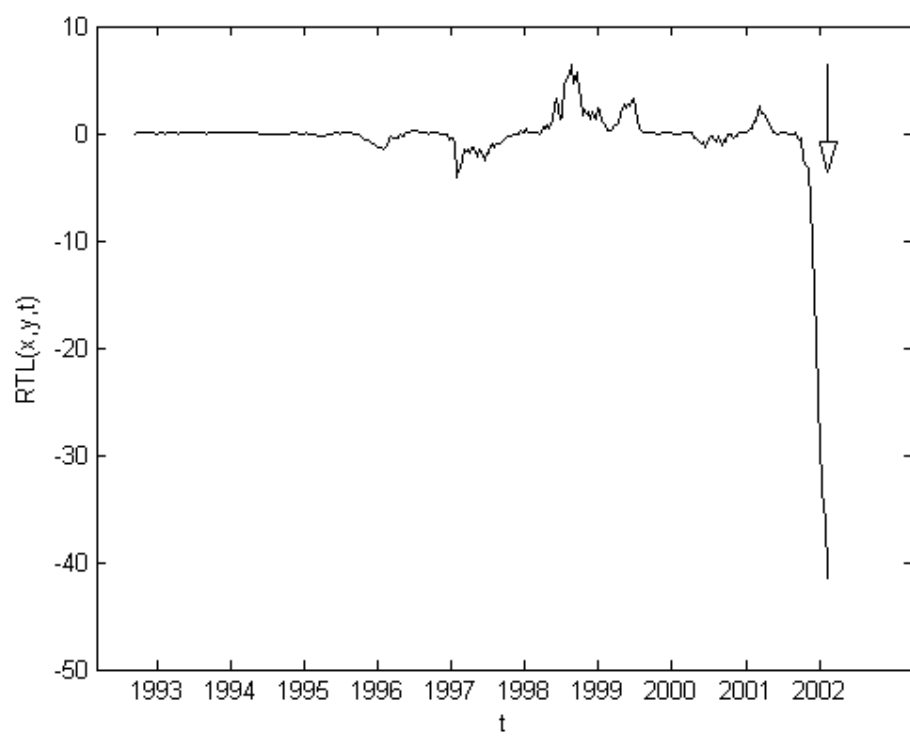
(a)



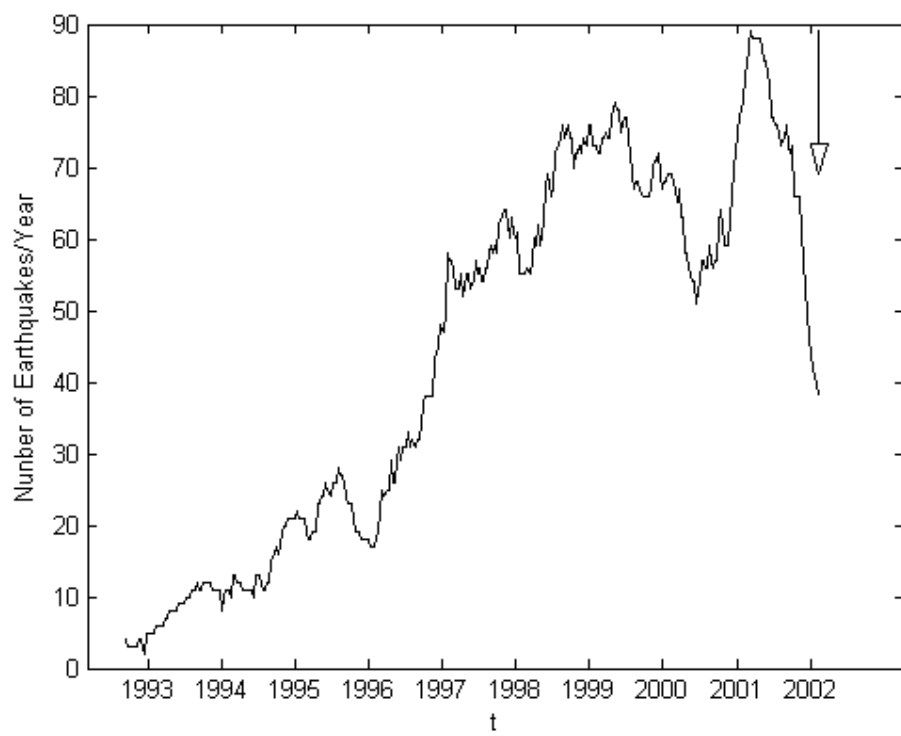
(b)

Fig. 4



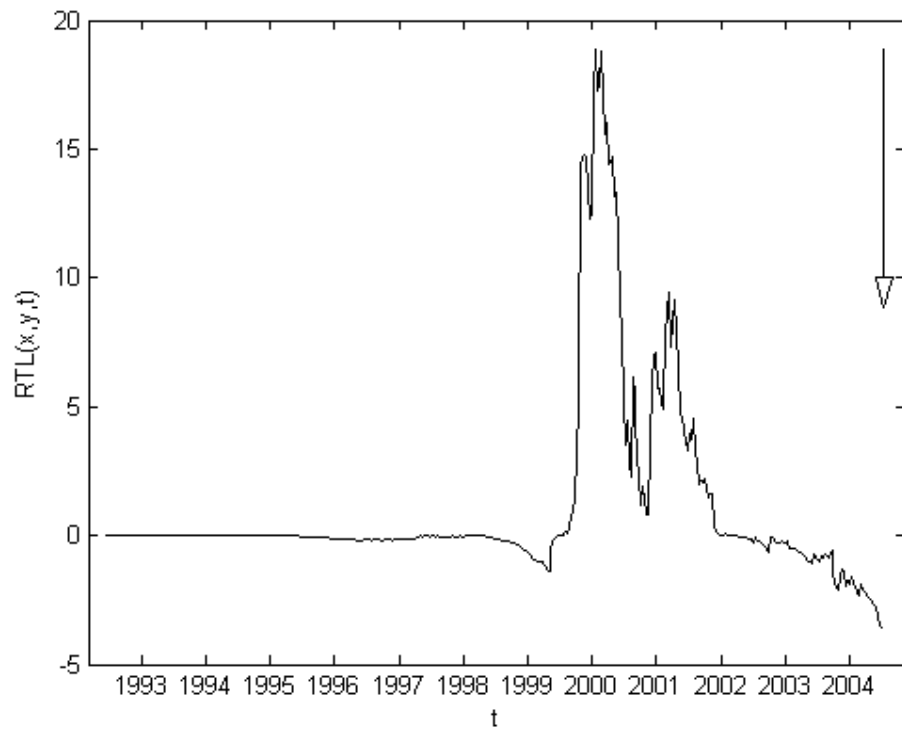


(a)

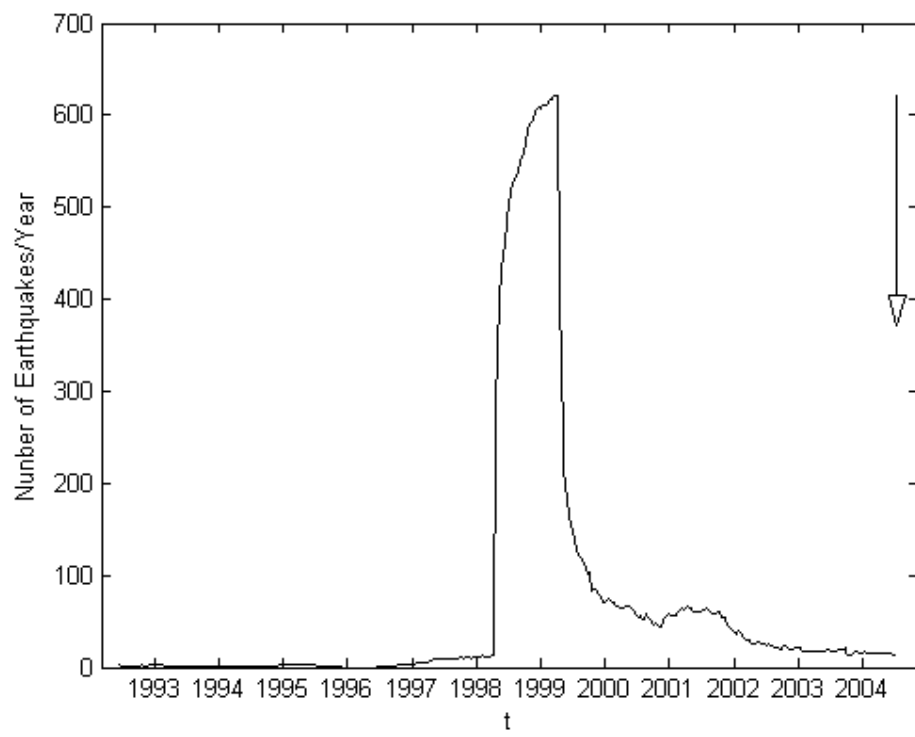


(b)

Fig. 6



(a)



(b)

Fig. 7

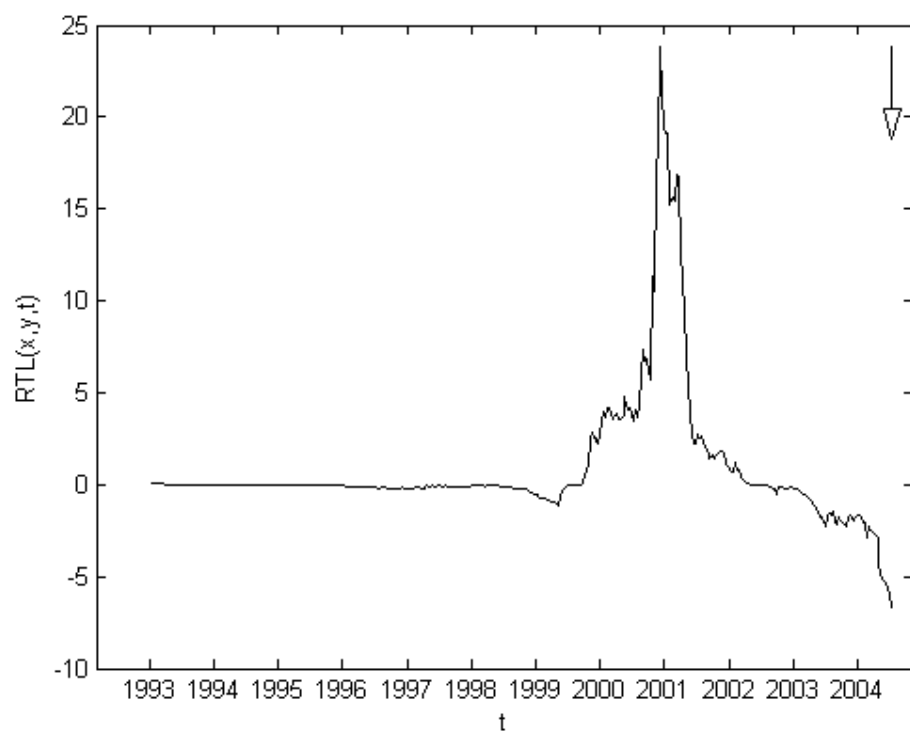
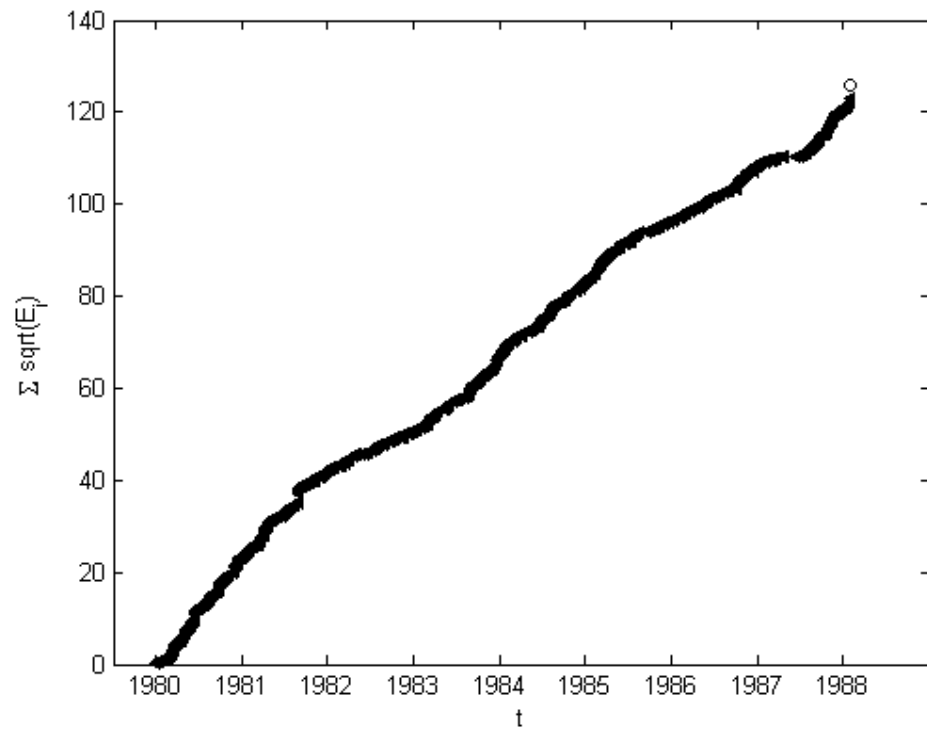
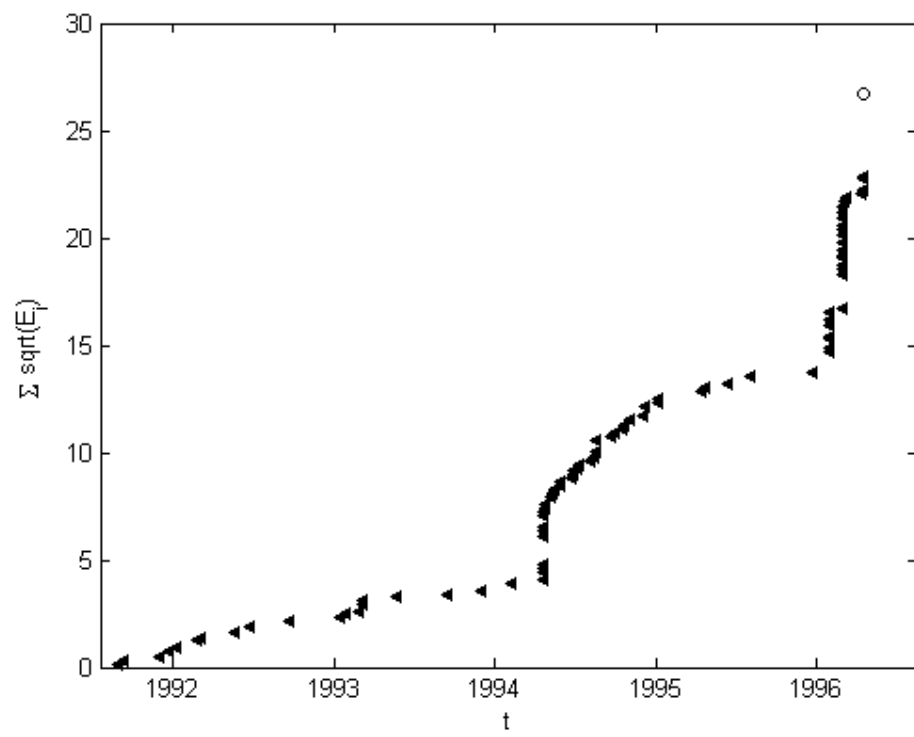


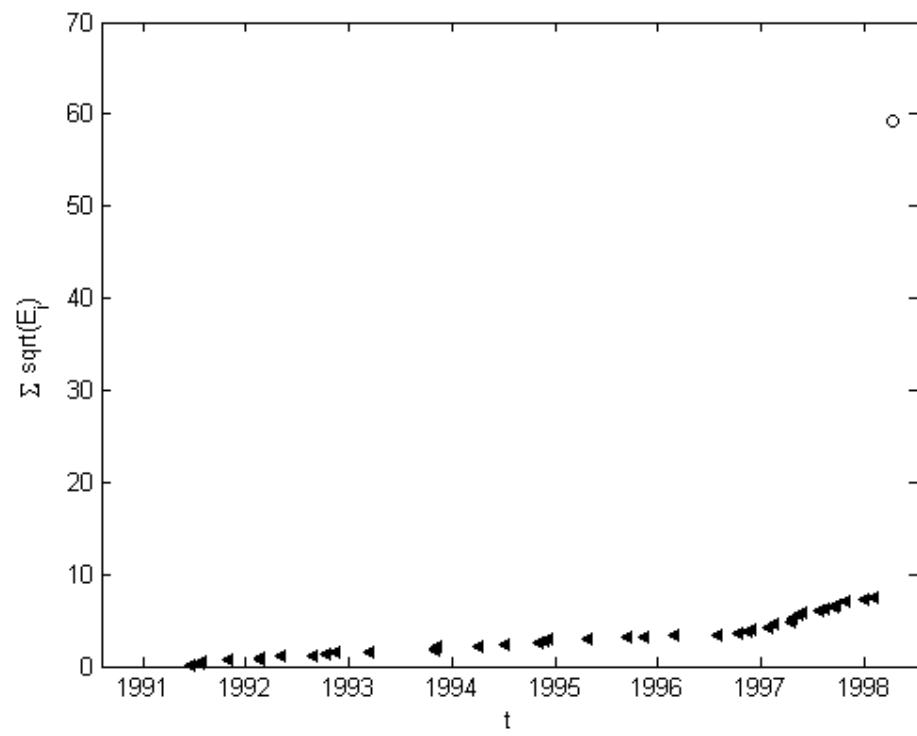
Fig. 8



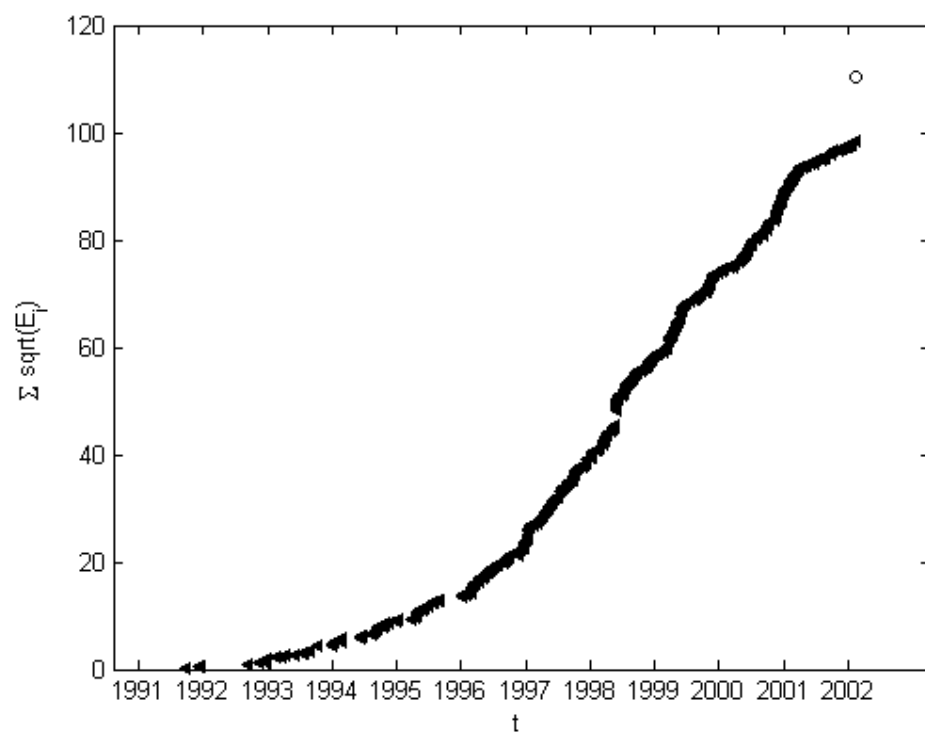
(a)



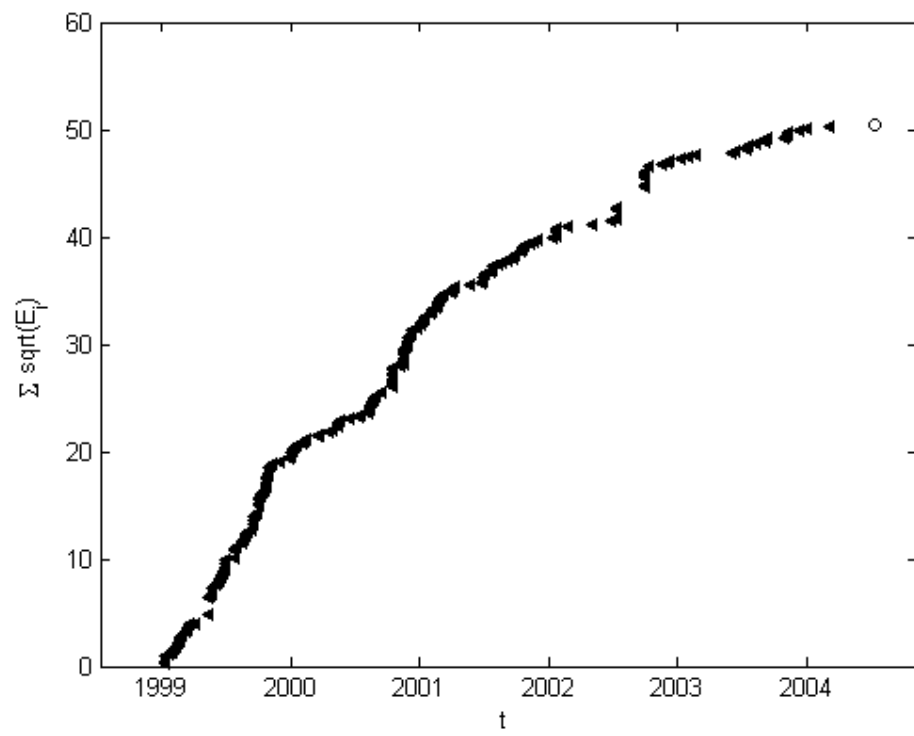
(b)



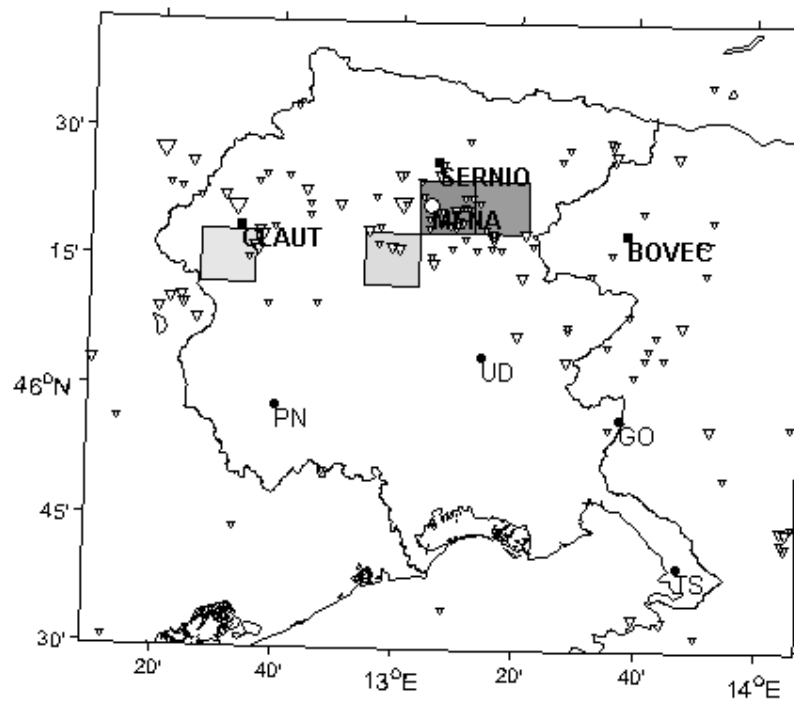
(c)



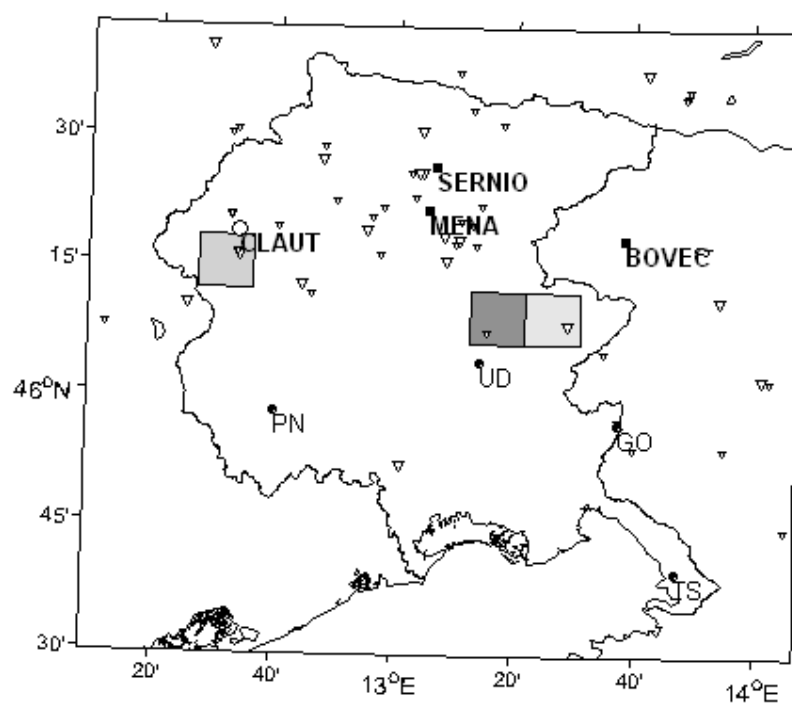
(d)



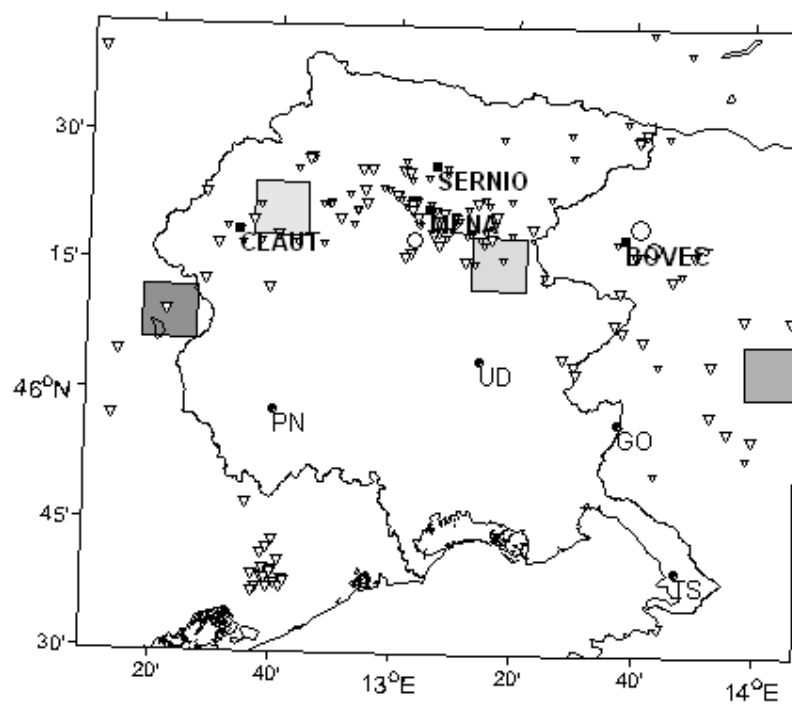
(e)
Fig. 9



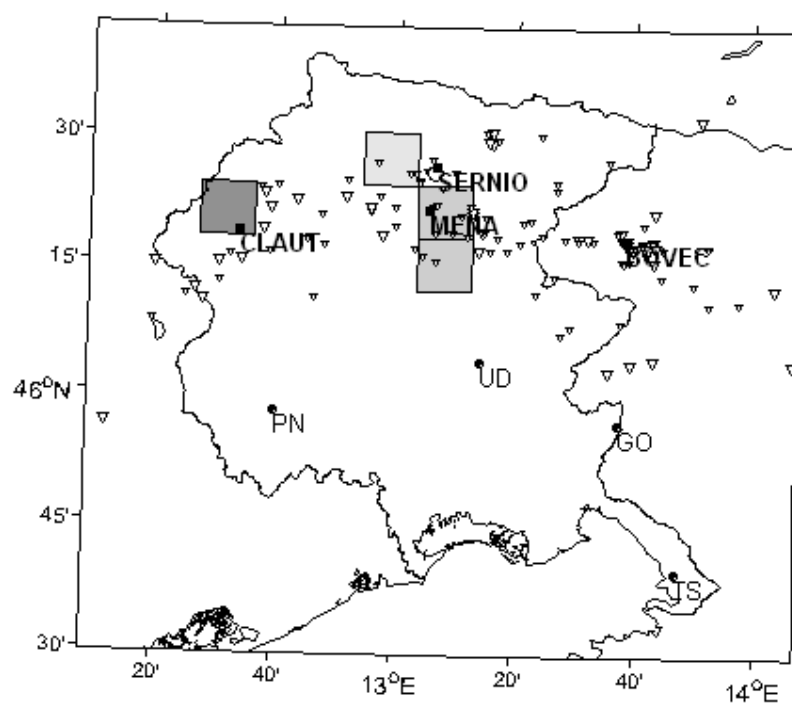
(a)



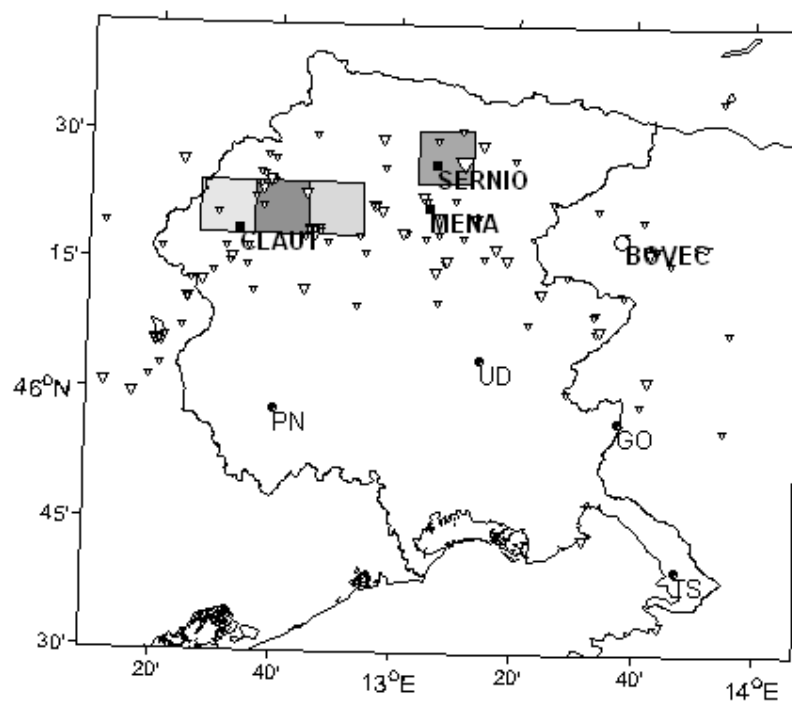
(b)



(c)



(d)



(e)

Fig 10

Tables

Earthquake	Case		Correlation coefficient
	A	B	
Bovec 2004	$r_0=20\text{km}$	$r_0=30\text{ km}$	0.99
		$r_0=10\text{km}$	0.94
		$r_0=5\text{ km}$	0.91
Sernio	$r_0=20\text{km}$	$r_0=30\text{ km}$	0.99
		$r_0=10\text{km}$	0.56
		$r_0=5\text{ km}$	0.21
Bovec 1998	$r_0=20\text{km}$	$r_0=30\text{ km}$	0.76
		$r_0=10\text{km}$	0.70
		$r_0=5\text{ km}$	N. A.
Claut 96	$r_0=20\text{km}$	$r_0=30\text{ km}$	0.84
		$r_0=10\text{km}$	0.97
		$r_0=5\text{ km}$	0.95
Mena	$r_0=20\text{km}$	$r_0=30\text{ km}$	0.93
		$r_0=10\text{km}$	0.58
		$r_0=5\text{ km}$	0.47

Table 1

Earthquake	Case		Correlation coefficient
	A	B	
Bovec 2004	$M_c=3.8$	$M_{\max}=\infty$	1
		$M_{\max}=M_{\text{seq}}-2$	0.95
Sernio	$M_c=3.8$	$M_{\max}=\infty$	1
		$M_{\max}=M_{\text{seq}}-2$	0.98
Bovec 1998	$M_c=3.8$	$M_{\max}=\infty$	1
		$M_{\max}=M_{\text{seq}}-2$	1
Claut 96	$M_c=3.8$	$M_{\max}=\infty$	1
		$M_{\max}=M_{\text{seq}}-2$	0.95
Mena	$M_c=3.8$	$M_{\max}=\infty$	1
		$M_{\max}=M_{\text{seq}}-2$	0.82

Table 2

Earthquake	Case		Correlation coefficient
	A	B	
Bovec 2004	$t_0=0.5\text{ years}$	0.8 years	0.54
Sernio	$t_0=0.5\text{ years}$	0.2 years	0.56
Bovec 1998	$t_0=0.5\text{ years}$	0.7 years	0.73
Claut 96	$t_0=0.5\text{ years}$	0.3 years	0.66

Table 3